Synchrotron X-Ray Studies of Short-Range-Order Iron and Manganese Oxides as Intercalation Cathodes for Rechargeable Lithium Batteries

Gaurav Jain[1], Mahalingam Balasubramanian[2], Jingsi Yang[1], Jun John Xu[1]

[1]Rutgers, The State University of New Jersey, Piscataway, NJ; [2]X.F.D., APS, Argonne National Laboratory, Argonne, IL

Introduction

Nanostructured materials as intercalation electrodes for rechargeable lithium batteries have recently attracted significant attention. Nanostructured, amorphous or nanocrystalline forms of various cathode materials have been reported to yield dramatically different (improved) electrochemical properties than their crystalline counterparts. This reported outlines our work on the study of these nanostructured intercalation host materials by synchrotron x-ray absorption spectroscopy (XAS). The weak structural ordering in these materials renders characterization using conventional x-ray diffraction rather difficult. On the other hand, investigations using synchrotron XAS can yield a wealth of structural information critical to understanding the intercalation mechanisms and structure-property relationships in these materials. The XAS measurements can be carried out in situ [1], namely, in a spectro-electrochemical cell while the discharge-charge process is going on. These experiments have been the focus of this work.

Methods and Materials

Materials Synthesis: The synthesis of the nanostructured materials of this study has been conducted at the Department of Ceramics and Materials Engineering, Rutgers University. The compounds were synthesized via low temperature, aqueous precipitation routes or aqueous sol-gel routes [2-3]. The reactions products are obtained by freeze drying the reaction precipitates/gel, followed by moderate heat-treatment at 250-400ºC.

X-ray Absorption Spectroscopy Measurements: X-ray absorption spectroscopy experiments (XAS) were performed in the PNC-XOR bending magnet beamline (20-BM) of the Advanced Photon Source at the Argonne National Laboratory, IL, USA. Measurements at the iron/manganese K-edge were performed in the transmission mode using gas ionization chambers to monitor the incident and transmitted x-ray intensities. A third ionization chamber was used in conjunction with an iron/manganese standard to provide internal calibration for the alignment of the edge positions. A pair of Si (111) crystals was used to monochromatize the radiation. A rhodium-coated x-ray mirror was utilized to suppress higher order harmonics. In situ XAS studies to monitor the electronic and structural changes of the cathode material were performed using a specially designed spectro-electrochemical cell in which the x-ray beam is allowed to pass through the cell, while the discharge-charge cycling is conducted. A detailed construction of the cell is given elsewhere [1].

Results

Nanostructured Iron Oxide: The nanocrystalline-Fe_2O_3, that we have synthesized exhibits electrochemical properties dramatically superior to those of microcrystalline α-Fe_2O_3. The material delivers highly reversible specific capacities of 200-250 mAh/g and energy densities of 425-500 mWh/g, at different current rates [2]. Under similar conditions the microcrystalline α-Fe_2O_3 is known to display nearly inactive electrochemical behavior as a cathode material, with specific capacities of 25-45 mAh/g [4-5].

The structural behavior of the microcrystalline α-Fe_2O_3, upon lithium intercalation has been previously investigated [4-5]. The objective of the current work is to establish the structural behavior of the nanocrystalline-Fe_2O_3 and understand the differences over the microcrystalline compound. Firstly, a change in the oxidation state of Fe is expected if Faradaic processes occur during electrochemical discharge and charge. X-ray absorption near edge spectrosocpy (XANES) analysis is employed to track changes and the reversibility in Fe oxidation state during discharge and charge. Further, the phase transformation behavior of the compound needs exploration. The microcrystalline α-Fe_2O_3 is known to undergo transformation from a hexagonal R-3C structure to a cubic structure upon intercalation of < 0.1 Li/Fe_2O_3 [4-5]. The overall reversible intercalation capacity delivered by the nanocrystalline-Fe_2O_3 shows a capacity of ca. 1.4 Li/Fe_2O_3. How this lithium is accomodated into the structure and what changes the structure undergoes, need to be ascertained.

XAS results were obtained for the as-prepared nanocrystalline-Fe_2O_3 and microcrystalline-Fe_2O_3 samples, along with that for various iron oxide standard compounds. Fig. 1 shows the XANES spectra of the as-prepared nanocrystalline-Fe_2O_3 and the microcrystalline-Fe_2O_3 samples. The nanocrystalline-Fe_2O_3 sample shows strong similarity in the edge structure and the position of the absorption edge to that for the microcrystalline-Fe_2O_3, which corresponds very well to that reported for α-Fe_2O_3. The pseudo radial distribution function (RDF) in the Fig. 2 shows the various coordination shells around a Fe atom. The peaks seen for the nanocrystalline-Fe_2O_3 and the microcrystalline-Fe_2O_3 correspond very well with those expected for the various face-shared, edge-shared and corner-shared linkages for the α-Fe_2O_3 structure. Detailed quantitative analysis indicates certain defects associated with the nanocrystalline-Fe_2O_3 sample, corresponding to presence of oxygen vacancies in the second Fe-O shell and Fe vacancies in some of the Fe-Fe shells [6].

In situ XAS measurements were conducted during discharge and charge of the cell containing the nanocrystalline-Fe_2O_3 cathode. The cell was cycled at a 10 hour discharge/charge rate. A total of 22 scans were collected continuously during the first discharge. A specific capacity of 230 mAh/g, equivalent to intercalation of 1.36 Li/Fe_2O_3, was obtained in this discharge. Selected XANES spectra from scans 1-22 are shown in Fig. 3. These show a total shift of 2.3 eV in the edge position during discharge. The absorption edge for the fully discharged sample lies between that of the Fe_3O_4 and FeO standard, signifying that the oxidation state of Fe must be between +2.5 and +2, showing good agreement with the expected change in Fe oxidation state. Upon charging, the edge shows systematic movement towards higher energies, signifying Faradaic oxidation and good reversibility of the compound (not shown here).

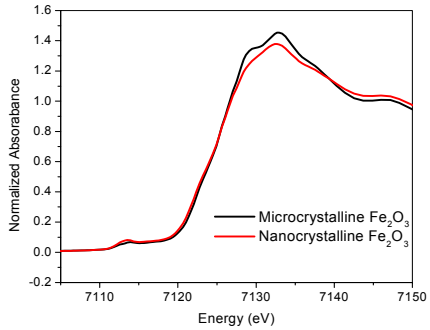

Fig. 1. XANES data of the as-prepared nanocrystalline-Fe_2O_3 and microcrystalline-Fe_2O_3.

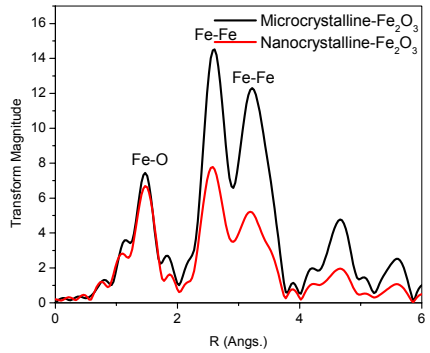

Fig. 2. Pseudo-RDF pattern of the as-preapred nanocrystalline-Fe_2O_3 and microcrystalline-Fe_2O_3

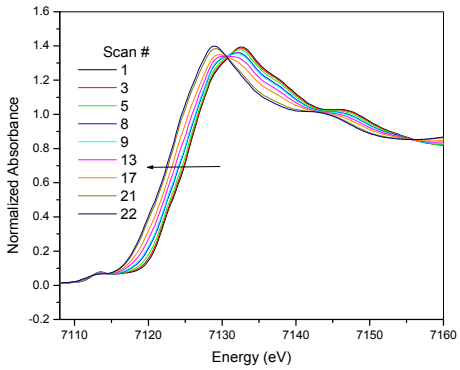

Fig. 3. XANES data for the scans 1-22 for the first discharge for the nanocrystalline-Fe_2O_3. Data shows systematic shift in edge position as evidence of Faradaic reduction during discharge.

Detailed analysis of the XAS data for the nanocrystalline-Fe_2O_3 obtained during discharge, indicate distinctive behavior of the material during the scans 1-7 and the scans 8-22. The scans 8-22 (Fig.4(b)), show unique common intersection points or a single set of isosbestic points through the spectra. On the other hand, scans 1-7 do not show any unique common intersection points with the other scans (Fig. 4(a)). Presence of a single set of isosbestic points in the spectra is an indication of occurrence of a two-phase reaction [7]. The cathode material during the scans 8-22 appears to be composed of two phases, one with lower lithium content than the other. As discharge proceeds, the amount of the latter phase must increase at the expense of the former. The measured XANES spectra during these scans are linear combinations of the XANES spectra of these two phases and thus always show common intersection points. During the scans 1-7 the material does not seem to undergo a two-phase reaction and instead appeas to allow single phase intercalation. The single phase capacity corresponding to the 8th scan amounts to intercalation of 0.47 Li/Fe_2O_3. This single phase intercalation capacity is substantially higher than that reported for microcrystalline α-Fe_2O_3, which is known to undergo transformation to a cubic structure for less than 0.1 Li in the hexagonal structure.

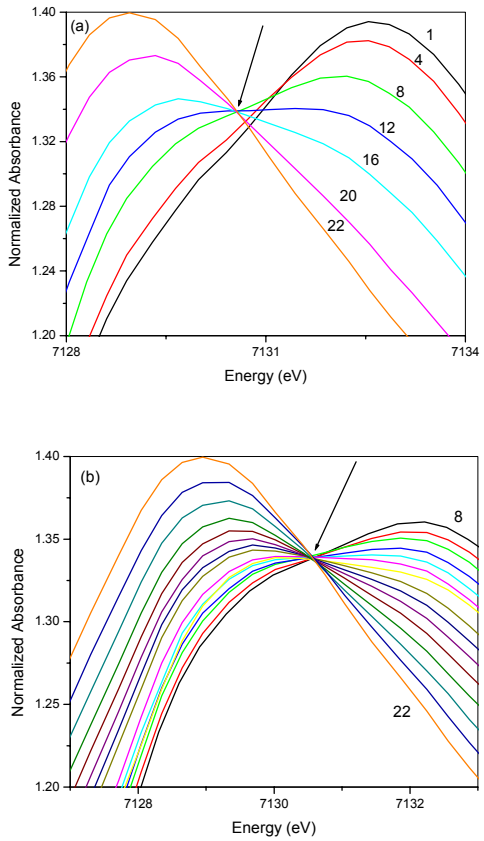

Fig. 4. XANES data for scans 1-22 (a) Expanded view of the main peak at the edge for selected scans between 1-22. (b) Expanded view of the main peak at the edge for scans 8-22. Note the presence of a common intersection point (isosbestic point) for scans 8-22. Scans 1-7 do not intersect the other scans at any unique common intersection point. In both figures the arrow points to the isosbestic point seen for scans 8-22.

Principal component analysis is being conducted to isolate the contributions of the different coexisting components contributing to the 8th-22nd spectra. The XAS spectra for the two phases extracted from the data and a detailed analysis will be reported shortly [6].

Nanocrystalline Lithium Manganese (IV) Oxide: The nanocrystalline lithium manganese oxide that we have synthesized via a sol-gel route (LMO-400º) possesses a composition close to Li_2MnO_3. Li_2MnO_3 is known to have a rock salt, monoclinic structure, in which octahedrally coordinated cations are arranged in alternating layers of Li and $LiMn_2$. Conventionally, Li_2MnO_3 is reported to be electrochemically inactive as a lithium intercalation host [8].

Lithium cannot be extracted from this compound since Mn is already in 4+ oxidation state. Lithium cannot be inserted into this compound since all octahedral sites are filled. The results obtained for our nanocrystalline Li_2MnO_3-like compound show suprising electrochemical activity. The as-prepared compound allows reversible intercalation of up to 0.87 Li/Mn. The compound also shows excellent electrochemical reversibility. XRD after dischage and charge indicates that the long-range structure of the compound does not change during intercalation/deintercalation. XAS evaluation of this material is critical to understanding the structure of the as-prepared material and it's behavior upon discharge/charge. Firstly, a similarity of the local structure of the as-prepared LMO-400º sol-gel sample to that of rock-salt Li_2MnO_3 needs to be established. Next, it must be ascertained via XANES whether the intercalation and deintercalation processes show corresponding changes in Mn oxidation state in the compound.

Extended x-ray absorption fine structure spectroscopy (EXAFS) data of the LMO-400º sample and manganese oxide standard compounds such as the spinel $LiMn_2O_4$, $Li_4Mn_5O_{12}$ and rock-salt Li_2MnO_3 were obtained (not shown here). Close inspection of the data reveals significant difference between the LMO-400º sample and the spinels. On the other hand, comparisons of the LMO-400º data with the Li_2MnO_3 clearly indicate that the medium range structure around Mn in the sample is similar to that around Mn in Li_2MnO_3. The data does show indication of less crystalline and more disordered nature of the the LMO-400º sample.

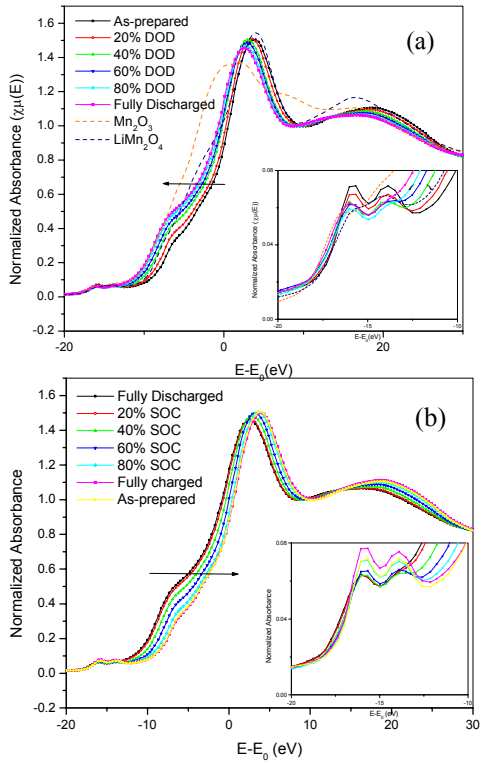

Fig. 5. In situ XANES spectra of the sol-gel sample obtained during discharge (a) and charge (b) of the material showing Faradaic reduction and oxidation of Mn.

In situ XANES data were obtained for the LMO-400º sample (Fig. 5) using the spectro-electrochemical cell described before. XAS scans were collected continuously during discharge and charge of the sample at a rate close to C/10. The discharge capacity obtained was ca. 191 mAh/g, equivalent to intercalation of 0.83 Li per Mn. The consecutive XANES scans (Fig. 5(a)) show a continuous, systematic lowering of the edge position along with the discharge, signifying a clear decrease in the Mn oxidation state. The edge shows a rigid movement during discharge, with a total decrease in the edge energy of ca. 2.1 eV. The XANES spectrum for the fully discharged state, shows an absorption edge position significantly lower than $LiMn_2O_4$ ($Mn^{3.5+}$) spectra but closer to Mn_2O_3 (Mn^{3+}), in agreement with the expected average oxidation state of 3.17+. These data clearly show a Faradaic decrease in the Mn oxidation state during discharge, and show no evidence of any significant amount of non-Faradaic processes occurring in the cell. Upon charging, the sample shows perfect electrochemical reversibility. Charging XANES scans show (Fig. 5(b)) that the material undergoes oxidation and shows complete reversibility in terms of Mn oxidation state. Detailed structural analysis shows that the material shows excellent local structure reversibility as well [9]. This electrochemical performance of the nanocrystalline Li_2MnO_3 is indeed surprising. Investigation via NMR are being conducted to complement the XAS study and ascertain the sites that Li occupies in this close packed structure.

Acknowledgement

The authors thank Dr. James McBreen and Dr. Won-sub Yoon for their help with the XAS study. This work is supported by the NSF Industry/University Collaborative Research Center on Ceramic and Composite Materials at Rutgers University/Penn State University/University of New Mexico. Partial support of the Office of Naval Research is gratefully acknowledged. PNC-CAT facilities at the Advanced Photon Source, and research at these facilities, are supported by the US DOE Office of Science Grant No. DEFG03-97ER45628, the University of Washington, a major facilities access grant from NSERC, Simon Fraser University and the Advanced Photon Source. Use of the Advanced Photon Source is also supported by the U. S. Department of Energy, Office of Science, Office of Basic Energy Sciences, under Contract No. W-31-109-Eng-38.

References

1. M. Balasubramanian, X. Sun, X. Q. Yang and J. McBreen, J. Power Sources, 92, 1 (2001).
2. J. J. Xu, G. Jain, Electrochem. & Solid- State Lett,, **6**, A190 (2003).
3. J. Yang, J. J. Xu, J. Power Sources, **122**, 181 (2003).
4. M. M. Thackeray, W. I. F. David, J. B. Goodenough, Mat. Res. Bull., **17** 785 (1982).
5. D. Larcher, C. Masquelier, D. Bonnin, Y. Chabre, V. Masson, J.-B. Leriche and J.-M. Tarascon, J. Electrochem. Soc., **150**, A133 (2003).
6. G. Jain, M. Balasubramanian, J. J. Xu, Chem. Mater., to be submitted.
7. M. Balasubramanian, J. McBreen, X. –Q. Yang, S. Khalid, K. Zaghib, Abs. No. Bala0313, *Activity Rep.*, NSLS, BNL (2002).
8. M. M. Thackeray, Prog. Solid St. Chem., 25, 1-71 (1997).
9. G. Jain, J. Yang, M. Balasubramanian, J. J. Xu, Chem. Mater., to be submitted.